NMR Calculations for Paramagnetic Molecules and Metal Complexes

Jochen Autschbach

Department of Chemistry, University at Buffalo,
State University of New York, Buffalo, NY 14260-3000, USA

email: jochena@buffalo.edu

published in *Annu. Rep. Comput. Chem.* 11 (2015), 3–36

Abstract: Molecules and metal complexes with paramagnetic ground states or low-energy paramagnetic electronic excited states may exhibit profound effects due to electron paramagnetism on NMR parameters such as nuclear magnetic shielding constants and indirect nuclear spin-spin coupling. This review discusses different approaches that can be used to calculate such effects from first principles, either with or without employing fictitious spin Hamiltonian parameters. Case studies are presented, along with an overview of selected recently published computational studies of NMR chemical shifts of paramagnetic systems.

Keywords: NMR shifts, electron paramagnetism, ab-initio theory, density functional theory, relativistic effects, hyperfine coupling

1 Introduction

Molecules and metal complexes with unpaired electrons may exhibit pronounced electron paramagnetism. Such systems can be characterized experimentally by exploiting the paramagnetism specifically, for instance via measurements of the magnetic susceptibility or electron paramagnetic resonance (EPR) spectra. Paramagnetic effects may also affect the nuclear magnetic shielding tensors, the isotropic shielding, the chemical shifts, and indirect nuclear spin-spin coupling ($\boldsymbol{J}$-coupling), in nuclear magnetic resonance (NMR) spectroscopy. The acronym pNMR is used in herein in reference to NMR of paramagnetic systems, or the effects on NMR parameters that are specific to the electron paramagnetism. If the latter leads to too fast relaxation of the nuclear spins, it can be difficult to obtain NMR signals experimentally. However, many experimental studies of paramagnetic species report – often well resolved – NMR spectra where pNMR effects are evident. Unfortunately, the interpretation and assignment of such spectra can be challenging. Consequently, there is a demand for quantum chemical methods and protocols that are suitable for predicting and analyzing pNMR data.

Norman Ramsey published the nonrelativistic theory for NMR shielding for diamagnetic systems starting in 1950 [1]. Eight years later, McConnell and Chesnut [2] derived the EPR spin Hamiltonian term that is bi-linear in the nuclear spin magnetic moment and the external magnetic field, which is in essence the term responsible for the pNMR shift. This formulation has been used for many pNMR chemical shift calculations ever since. In the inorganic chemistry and organometallic chemistry communities, there are also corresponding crystal-field (CF) theory based models for pNMR shifts available [3–5] that remain in use. Previous derivations in terms of *ab-initio* theory were put forward, for instance, by Kurland and McGarvey in 1970 [6], by Rinkevicius et al. [7] in 2003, and by Moon and Patchkovskii [8] in 2004 who provided the first complete general theoretical formulation and suggested a computational protocol in terms of EPR parameters. We forego a detailed historical perspective or a comprehensive account of theoretical methods that have been proposed over time and their applications. A textbook chapter by Vaara [9] and the Moon & Patchkovskii book chapter [8] cover much of the relevant relevant older literature, and Vaara summarizes many of the computational studies available up to ca. 2012. The theory section in Vaara's book chapter emphasizes various contributions to the pNMR shielding tensor that can be defined in the leading order of relativistic effects, which the reader might find instructive.

Recent years have witnessed redoubled efforts to establish reliable yet practical theoretical approaches, which therefore warrants a short review. We focus on chemical shifts because pNMR effects on other NMR parameters are essentially unexplored computationally, but an equation for $\boldsymbol{J}$-coupling is provided for completeness. As already pointed out, for a long time, pNMR shifts

have been expressed predominantly in terms of EPR spin Hamiltonian parameters or spin susceptibilities, and calculations were used to determine these quantities to estimate pNMR shifts. Only recently has the focus shifted to what may be termed 'direct' methods, i.e. calculations without recourse to EPR parameters or magnetic susceptibilities. We take the opportunity to outline a derivation by Soncini and van den Heuvel (SvH) [10, 11], published in 2013 with a 2012 precursor [12], for the pNMR shielding tensor in an *ab-initio* framework and how the EPR parameter-based spin Hamiltonian formulation is obtained from it. We recently reported the, to our knowledge, first direct *ab-initio* pNMR shift calculation [13]. The application to two actinide complexes also demonstrated that the SvH formalism is compatible with a relativistic quantum chemistry framework [14–16], which is crucial for systems with heavy elements.

Section 2 outlines the theory, and Section 3 discusses selected case studies utilizing EPR parameter- and magnetic susceptibility-based calculations as well as the direct framework. Concluding remarks and an outlook can be found in Section 4.

2 Theory

We sketch the derivation by Soncini and van den Heuvel (SvH) for the nuclear magnetic shielding tensor as a temperature- (T-) dependent bi-linear derivative of the Helmholtz free energy [10, 11], using the notation of a recent paper by our group [17].

The bi-linear derivative of the Helmholtz free energy F is

$$\sigma_{ij}^{N}(T) = \frac{\partial^2 F}{\partial B_i \partial \mu_j^N} \tag{1}$$

Here, $i, j \in \{x, y, z\}$, N is the nucleus of interest, μ_i^N is a component of the nuclear spin magnetic moment vector $\boldsymbol{\mu}^N$, and B_i is a component of the external magnetic field vector $\boldsymbol{B}$. The derivatives are understood to be taken at $\boldsymbol{B} = 0, \boldsymbol{\mu}^N = 0$. The result, σ_{ij}^N, is a component of the nuclear magnetic shielding tensor $\boldsymbol{\sigma}^N$ in its Cartesian representation. The isotropic shielding constant is $\sigma_N = (1/3)\,\mathrm{tr}[\boldsymbol{\sigma}]$, where 'tr' is the matrix trace (sum of diagonal elements).

In a quantum mechanical framework, calculating a bi-linear derivative (a double-perturbation

molecular property [18]) requires the linear and bi-linear derivatives of the Hamiltonian $\hat{H}$:

$$\hat{H}^{\mathrm{HyF}}_{Ni} = \frac{\partial \hat{H}}{\partial \mu^N_i} \tag{2a}$$

$$\hat{H}^{\mathrm{Z}}_{i} = \frac{\partial \hat{H}}{\partial B_i} \tag{2b}$$

$$\hat{H}^{\mathrm{DS}}_{Nij} = \frac{\partial^2 \hat{H}}{\partial B_i \partial \mu^N_j} \tag{2c}$$

The term in (2a) is the hyperfine (HyF) operator component i for nucleus N describing the perturbation of the molecule by the presence of the nuclear spin magnetic moment, (2b) is the electronic magnetic moment operator operator component i describing the Zeeman (Z) interaction with a static external magnetic field, and the bi-linear derivative (2c) is the diamagnetic shielding (DS) operator component i, j for nucleus N. Note that SvH defined the operator linear in the external field explicitly with a negative sign. Below, this would change the signs of the terms that are bi-linear in the first-order operators. [In References 17 and 13 we used a similar notation as SvH but missed writing the negative sign in the equation corresponding to (2b) in Reference 17.] The electronic Hamiltonian in the absence of perturbations by the external field and the HyF field is

$$\hat{H}_0 = \sum_{\lambda,a} E_\lambda |\lambda a\rangle\langle \lambda a| \tag{3}$$

The normalized eigenfunctions $|\lambda a\rangle$ corresponding to the energies E_λ carry an index a to count the components of degenerate states. For convenience, the components of a degenerate state are assumed to to be mutually orthogonal. SvH carried out a thermal average in the canonical ensemble corresponding to $\hat{H}_0$ to arrive at the shielding tensor elements in a sum-over-states (SOS) formulation:

$$\sigma^N_{ij}(T) = \frac{1}{Q}\sum_\lambda e^{-\frac{E_\lambda}{k_B T}}\Big[\sum_a \langle \lambda a|\hat{H}^{\mathrm{DS}}_{Nij}|\lambda a\rangle - 2\,\mathrm{Re}\sum_{\lambda'\neq\lambda}\sum_{a,a'}\frac{\langle \lambda a|\hat{H}^{\mathrm{Z}}_i|\lambda' a'\rangle\langle \lambda' a'|\hat{H}^{\mathrm{HyF}}_{Nj}|\lambda a\rangle}{E_{\lambda'}-E_\lambda} - \frac{1}{k_B T}\sum_{a,a'}\langle \lambda a|\hat{H}^{\mathrm{Z}}_i|\lambda a'\rangle\langle \lambda a'|\hat{H}^{\mathrm{HyF}}_{Nj}|\lambda a\rangle\Big] \tag{4}$$

In Equation (4), $Q = \sum_{\lambda,a}\exp(-E_\lambda/(k_B T))$ is the partition function in the absence of the external and HyF fields, and k_B is the Boltzmann constant. The following points are emphasized:

1. For a non-degenerate ground state (GS), negligible Boltzmann populations of excited states, and for a nonrelativistic quantum mechanical framework, Equation (4) gives the Ramsey shielding [1]. Ramsey also wrote his shielding expression in SOS form.

2. In Reference 1, Ramsey stated correctly that his methods 'could be generalized to include the electron spin explicitly' and suggested an approach along the lines of Van Vleck [19]. However, Ramsey's statement that 'the magnetic shielding fields from the electron spin should be of a higher order of smallness than the other contributions' turned out to be incorrect if he was referring to paramagnetic systems, or even closed-shell systems if they contain heavy atoms. Examples are discussed in Section 3 where the Ramsey contributions to the isotropic shielding are small in comparison to those caused by the electron spin. For light-element closed-shell systems, Ramsey's assessment that electron spin dependent terms in the Hamiltonian can be neglected for NMR shielding calculations is certainly valid.

3. The replacements

$$\hat{H}^{\mathrm{HyF}}_{Nj} \rightarrow \hat{H}^{\mathrm{Z}}_{j}$$
$$\hat{H}^{\mathrm{DS}}_{Nij} \rightarrow \hat{H}^{\mathrm{DM}}_{ij} = \frac{\partial^2 \hat{H}}{\partial B_i \partial B_j}$$

in Equation (4) give, up to a constant, the Van Vleck [19] equation for the components of the magnetic susceptibility tensor $\boldsymbol{\chi}(T)$, meaning that $\chi_{ij}(T) = -\mu_0(\partial^2 F)/(\partial B_i \partial B_j)$. Here, μ_0 is the magnetic constant, and $\hat{H}^{\mathrm{DM}}_{ij}$ is the diamagnetic magnetizability operator. The pNMR shielding expression must indeed follow from Van Vleck's derivation for the susceptibility if one considers the appropriate bi-linear perturbation instead. Ramsey derived a corresponding nonrelativistic SOS expression for diamagnetic molecules in 1952 [20].

4. The replacements

$$\hat{H}^{\mathrm{Z}}_{i} \rightarrow \hat{H}^{\mathrm{HyF}}_{Mi}$$
$$\hat{H}^{\mathrm{DS}}_{Nij} \rightarrow \hat{H}^{\mathrm{DSO}}_{MiNj} = \frac{\partial^2 \hat{H}}{\partial \mu^M_i \partial \mu^N_j}$$

in Equation (4) give an expression for the bi-linear perturbation of the energy by the magnetic moments of a pair of nuclei. This double perturbation represents the indirect (electron-mediated) NMR nuclear spin-spin coupling ($\boldsymbol{J}$-coupling) between nuclei M and N. Here, $\hat{H}^{\mathrm{DSO}}_{MiNj}$ is the diamagnetic spin-orbital operator. Ramsey derived the corresponding nonrelativistic SOS expression for diamagnetic molecules in 1953 [21].

5. Each term in the Boltzmann average in Equation (4) represents a static response function $\langle\langle \mu_i; B_j \rangle\rangle$ for state no. λ which can in principle be calculated by a variety of quantum chemical methods.

6. The Hamiltonian, the wavefunctions, and the response functions can be defined at different approximate levels of theory, using many electron wavefunctions of varying quality, and treating relativistic effects approximately or (one-electron-) exactly at the two-component level or at the four-component level. In the latter case, in its standard formulation there is no diamagnetic term, and the response functions include contributions from negative-energy states. In a density functional theory (DFT) framework, if there are low-energy excited states contributing to the Boltzmann average their contribution would need to be calculated as response functions of the excitation energies from a time-dependent DFT (TDDFT) approach (i.e. chemical shifts for the excited states), which entails calculations of non-linear response functions. Calculating excited state response from constricted-variational DFT [22, 23] is a potential alternative. Dealing with degenerate ground states in DFT with currently available approximate functionals is in itself not without problems, except for simple situations.

7. SvH referred for the last term on the right hand side of Equation (4), the one proportional to $1/k_B T$, as the Curie term. For non-degenerate states, the Curie term vanishes because the time-odd operators $\hat{H}_i^{\mathrm{Z}}$, $\hat{H}_{Nj}^{\mathrm{HF}}$ have no diagonal matrix elements.

8. For a degenerate magnetic ground state and absence of low-energy excited electronic states, the shielding tensor components have an intrinsic $1/T$ dependence from the Curie term. If the ground state is a spin multiplet, it may be split by zero-field splitting (ZFS) and a more intricate T-dependence may result, as discussed in detail in Reference 17. In a relativistic framework where the wavefunctions explicitly include effects from SO coupling and dipolar spin-spin interactions, the calculation already includes the ZFS in $\hat{H}_0$ and its eigenfunctions. A T-dependence that is different from $1/T$ may nonetheless arise from the Boltzmann averaging in Equation (4).

9. The second term on the right hand side of Equation (4) may be referred to as the linear response (LR) term [13], because it includes the SOS expression for the linear response of $|\lambda, a\rangle$ that is familiar from non-degenerate perturbation theory.

10. For an implementation of Equation (4) in terms of response functions, if a state is degenerate one should use state components diagonalizing one of the perturbations. In this case, Curie terms would not occur explicitly. Alternatively, it should be possible to calculate the Curie terms separately and exclude any contributions involving cross terms among components of state λ to its own response function.

The connection between the Curie and the LR terms becomes more clear if one assumes that the degeneracy of state λ is removed, as typically done in perturbation theory for degenerate states,

for instance by diagonalizing $\hat{H}_i^{\mathrm{Z}}$ within the subspace $|\lambda, a\rangle$. This creates linear combinations $|\mu^\lambda\rangle = \sum_a |\lambda, a\rangle U_{a\mu}$ with eigenvalues W_μ^λ (assumed to be non-degenerate) and new energies $E_\mu^\lambda = E_\lambda + W_\mu^\lambda$. The coefficients $U_{a,\mu}$ form a unitary matrix since the $|\lambda, a\rangle$ are assumed to be orthonormal. Suppose that the electronic energy gaps between λ' and λ as well as $k_B T$ are large compared to the W_μ^λ. The Boltzmann factor is approximately

$$e^{-\frac{E_\mu^\lambda}{k_B T}} \simeq e^{-\frac{E_\lambda}{k_B T}} \left(1 - \frac{W_\mu^\lambda}{k_B T}\right) \tag{5}$$

Apart from insignificant changes in the LR term (and in Q, if $\sum_\mu W_\mu^\lambda \neq 0$), instead of the Curie term for state λ, there is then an additional LR contribution

$$e^{-\frac{E_\lambda}{k_B T}} \sum_\mu \left(1 - \frac{W_\mu^\lambda}{k_B T}\right) 2\,\mathrm{Re} \sum_{\mu' \neq \mu} \frac{\langle \mu^\lambda | \hat{H}_i^{\mathrm{Z}} | \mu'^\lambda \rangle \langle \mu'^\lambda | \hat{H}_{Nj}^{\mathrm{HyF}} | \mu^\lambda \rangle}{W_{\mu'}^\lambda - W_\mu^\lambda} \tag{6}$$

When $\mu' \to \mu$ and $\mu \to \mu'$ in the restricted double sum, the energy denominator changes sign which eliminates the constant term from the expansion of the Boltzmann factor, while in the leftover a factor $W_{\mu'}^\lambda - W_\mu^\lambda$ cancels the energy denominator. In order to keep the full double sum, a factor of 1/2 is introduced, which gives from (6)

$$e^{-\frac{E_\lambda}{k_B T}} \frac{1}{k_B T} \sum_{\mu,\mu'} \langle \mu^\lambda | \hat{H}_i^{\mathrm{Z}} | \mu'^\lambda \rangle \langle \mu'^\lambda | \hat{H}_{Nj}^{\mathrm{HyF}} | \mu^\lambda \rangle \tag{7}$$

The case $\mu' = \mu$ can be included since $\hat{H}_{Nj}^{\mathrm{HyF}}$ should not have diagonal matrix elements in the eigenbasis of $\hat{H}_i^{\mathrm{Z}}$ that splits the degeneracy. Moreover, since the eigenfunctions of $\hat{H}_i^{\mathrm{Z}}$ within the degenerate subspace are given by a unitary transformation from the original set $|\lambda a\rangle$ one can transform back without changing the value of the double sum. Therefore, for a subset of states within the LR term for which the energies are close enough to each other such that the linearization of Equation (5) is valid, the contribution to the LR term from within the subset forms a Curie term.

Using the formalism as written, in a SOS framework, prevents a truly efficient calculation of the full shielding tensor because the wavefunction perturbations related to the HyF interactions, in particular, require many terms in the SOS to converge. In many application scenarios, however, one is interested in pNMR ligand chemical shifts in metal complexes where the only source of paramagnetism is a metal center (or several metal centers). The isotropic chemical shift of a given nuclear isotope in a probe with respect to the same isotope in a reference compound ('ref') is

$$\delta_N = \frac{\sigma_N^{\mathrm{ref}} - \sigma_N}{1 - \sigma_N^{\mathrm{ref}}} \simeq \sigma_N^{\mathrm{ref}} - \sigma_N \tag{8}$$

assuming that the shielding is in units of ppm; otherwise the right hand side includes a factor of 10^6. The approximation is usually very good because shielding constants are small. Suppose that pNMR effects in the shielding are separable as follows:

$$\sigma_N = \sigma_N^{\mathrm{orb}} + \sigma_N^{\mathrm{pNMR}} \tag{9}$$

Here, σ_N^{orb} represents the Ramsey shielding caused by magnetic field-induced orbital current densities which is sometimes referred to as 'orbital shielding', or a relativistic analog thereof which may also include the effects from field-induced spin-polarization. It is often assumed that a diamagnetic system that is chemically very similar to a paramagnetic probe system also has a very similar orbital shielding as the probe. The σ_N^{pNMR} term in the probe's shielding is then primarily caused by low-energy electronic states associated with the metal open shells, while shielding contributions in the SOS from high-energy states are expected to cancel in the chemical shift. These states related to the open shells may cause a permanent electronic magnetic moment and net spin density at the ligand atoms, which both give rise to pNMR effects. The analogous diamagnetic system is then used as a secondary NMR reference for the calculation. The chemical shift with respect to the 'official' (primary) reference can be obtained simply by adding the calculated or measured chemical shift of the nucleus in the secondary reference with respect to the primary reference. If both references are diamagnetic, the latter chemcical shift can be calculated by a variety of available quantum chemical methods for closed-shell systems.

Assuming that Equation (9) is valid and that the orbital shielding is similar in the probe and the diamagnetic secondary reference, the isotropic chemical shift is then dominated by

$$\delta_N^{\mathrm{pNMR}} = \sigma_N^{\mathrm{ref,dia}} - \sigma_N(T) = \frac{1}{3}\sum_i \frac{1}{Q}\sum_\lambda e^{-\frac{E_\lambda}{k_B T}} \times\Bigg[2\,\mathrm{Re}\sum_{\lambda'\neq\lambda}\sum_{a,a'}\frac{\langle\lambda a|\hat{H}_i^{\mathrm{Z}}|\lambda' a'\rangle\langle\lambda' a'|\hat{H}_{Ni}^{\mathrm{HyF}}|\lambda a\rangle}{E_{\lambda'}-E_\lambda} + \frac{1}{k_B T}\sum_{a,a'}\langle\lambda a|\hat{H}_i^{\mathrm{Z}}|\lambda a'\rangle\langle\lambda a'|\hat{H}_{Ni}^{\mathrm{HyF}}|\lambda a\rangle\Bigg] \tag{10}$$

where the sums now run over the manifold of electronic states associated with the metal open shells. Ideally, the chemical shift is obtained from the full shielding constants calculated via linear response functions without explicitly calculating excites states beyond those with non-negligible Boltzmann factors. In this case, the assumptions that Equation (9) is valid or that the orbital shieldings are transferable are not required.

Subsequent to the derivation of Equation (10), SvH invoked the EPR pseudo-spin Hamiltonian for $\hat{H}(\boldsymbol{\mu}^N, \boldsymbol{B})$ in order to make a connection with the pNMR theory most frequently used at the time. Spin Hamiltonian parameters can, of course, also be calculated from first principles. When a DFT framework is used and excited state contributions can be ignored, for instance, the EPR-based

route is computationally quite attractive, in particular since there are many different relativistic DFT implementations for EPR parameters available.

Let $\boldsymbol{I}^N$ be the nuclear spin vector. The relation with the nuclear spin magnetic moment is $\boldsymbol{\mu}^N = g_N \beta_P \boldsymbol{I}^N$, where β_P is the nuclear magneton and g_N the nuclear g-factor. Let $\hat{\boldsymbol{S}}$ be the electronic pseudo-spin vector operator. The EPR spin Hamiltonian to lowest order reads

$$\hat{H} = \hat{\boldsymbol{S}} \cdot \mathbf{D} \cdot \hat{\boldsymbol{S}} + \beta_e \boldsymbol{B} \cdot \mathbf{g} \cdot \hat{\boldsymbol{S}} + \hat{\boldsymbol{S}} \cdot \mathbf{A}^N \cdot \boldsymbol{I}^N \tag{11}$$

β_e is the Bohr magneton ($\beta_e = 1/2$ in atomic units). On the right hand side from left to right are the Hamiltonians for ZFS, the Zeeman interaction, and the hyperfine interaction, respectively. $\mathbf{D}$ is a 3×3 matrix parametrizing the ZFS, $\mathbf{g}$ is the 3×3 Zeeman coupling matrix ('g-tensor') parametrizing the Zeeman interaction, and $\mathbf{A}^N$ is the electron-nucleus hyperfine coupling matrix ('HyF' tensor') for nucleus N. Upright-bold notation is used to indicate matrices, and italic-bold is used for vectors. The multiplication dots indicate appropriate matrix-vector contractions to yield a scalar Hamiltonian. For the treatment of higher-order spin Hamiltonian parameters, see References 12 and 24.

In the EPR spin Hamiltonian framework, the field-free Hamiltonian and two of the perturbation operators of Equations (2) are given by

$$\hat{H}_0 = \hat{\boldsymbol{S}} \cdot \mathbf{D} \cdot \hat{\boldsymbol{S}} \tag{12a}$$

$$\hat{H}_i^{\mathrm{Z}} = \beta_e \sum_k g_{ik} \hat{S}_k \tag{12b}$$

$$\hat{H}_{Nj}^{\mathrm{HyF}} = \frac{1}{g_N \beta_P} \sum_k A_{kj}^N \hat{S}_k \tag{12c}$$

Consider a multiplet for spin S that is split by the zero-field interaction. Let the sets of eigenfunctions of $\hat{H}_0$ and the eigenvalues be $|S\lambda a\rangle$ and E_λ, respectively. For this multiplet, the shielding tensor elements of Equation (4) are given by

$$\sigma_{ij}^{\mathrm{pNMR}} = -\frac{\beta_e}{g_N \beta_P k_B T} \frac{1}{Q} \sum_{kl} g_{ik} A_{lj}^N \sum_\lambda e^{-\frac{E_\lambda}{k_B T}} \left[2k_B T \,\mathrm{Re} \sum_{\lambda' \neq \lambda} \sum_{a,a'} \frac{\langle S\lambda a|\hat{S}_k|S\lambda' a'\rangle\langle S\lambda' a'|\hat{S}_l|S\lambda a\rangle}{E_{\lambda'} - E_\lambda} + \sum_{a,a'} \langle S\lambda a|\hat{S}_k|S\lambda a'\rangle\langle S\lambda a'|\hat{S}_l|S\lambda a\rangle \right] \tag{13}$$

The EPR pseudo-spin Hamiltonian only describes the electron paramagnetism, and therefore the orbital shielding is not included in this formalism. A factor of $1/(k_B T)$ has been extracted from the λ-summation to emphasize the overall $1/T$ pre-factor of the paramagnetic shielding. The full

pNMR tensor can be written in a compact notation as

$$\boldsymbol{\sigma}^{\mathrm{pNMR}} = -\frac{\beta_{\mathrm{e}}}{g_N \beta_N k_B T}\, \mathbf{g}\, \mathbf{Z}\, \mathbf{A}^N \tag{14}$$

The elements of the 3×3 matrix $\mathbf{Z}$ are given by

$$Z_{kl} = \frac{1}{Q} \sum_{\lambda} e^{-\frac{E_\lambda}{k_B T}} \left[\sum_{a,a'} \langle S\lambda a | \hat{S}_k | S\lambda a' \rangle \langle S\lambda a' | \hat{S}_l | S\lambda a \rangle \right. \\ \left. + 2k_B T\, \mathrm{Re} \sum_{\lambda' \neq \lambda} \sum_{a,a'} \frac{\langle S\lambda a | \hat{S}_k | S\lambda' a' \rangle \langle S\lambda' a' | \hat{S}_l | S\lambda a \rangle}{E_{\lambda'} - E_\lambda} \right] \tag{15}$$

If the hyperfine spin Hamiltonian is written as $\boldsymbol{I} \cdot \mathbf{A}^N \cdot \hat{\boldsymbol{S}}$ instead of the reverse order used in Equation (11) then Equation (14) affords $(\mathbf{A}^N)^T$, the transpose of $\mathbf{A}^N$. The isotropic shielding in the EPR parameter-based framework is

$$\sigma^{\mathrm{pNMR}} = -\frac{\beta_{\mathrm{e}}}{g_N \beta_N k_B T}\, \frac{1}{3}\, \mathrm{tr}[\mathbf{g}\, \mathbf{Z}\, \mathbf{A}^N] \tag{16}$$

We note in passing that from an analogous derivation where the Zeeman operator is replaced with the hyperfine operator of a second nucleus, the corresponding expression for the paramagnetic effects on the reduced indirect spin-spin coupling tensor $\mathbf{K}$ for a pair of nuclei N, M would be

$$\mathbf{K}^{\mathrm{pNMR}}(M,N) = -\frac{1}{g_M g_N \beta_P^2 k_B T} (\mathbf{A}^M)^T\, \mathbf{Z}\, \mathbf{A}^N \tag{17}$$

The reduced spin-spin coupling can be converted to the J-coupling tensor in units of s^{-1} via

$$\mathbf{J}(M,N) = h \frac{\gamma_M}{2\pi} \frac{\gamma_N}{2\pi} \mathbf{K}(M,N) \tag{18}$$

Here, γ_N is a nuclear magneto-gyric ratio in rad/(T s), and h is Planck's constant ($\hbar = h/(2\pi)$). Note that $\hbar\gamma_N = g_N \beta_P$. Similar to the shielding, the pNMR J-coupling written in terms of EPR Hamiltonian parameters excludes other important contributions that require calculations by other means.

A treatment of ZFS effects in EPR parameter-based computations of pNMR shifts was described in 2007 by Hrobárik et al. [25]. Subsequently, a more rigorous approach to incorporate effects from ZFS in calculated pNMR shielding tensors within the EPR spin Hamiltonian frame-

work was proposed in Reference 26, which in our notation corresponds to letting

$$Z'_{kl} = \frac{1}{Q}\sum_{\lambda} e^{-\frac{E_\lambda}{k_B T}} \sum_{a} \langle S\lambda a|\hat{S}_k \hat{S}_l|S\lambda a\rangle \tag{19}$$

However, SvH later argued that Equation (19) is incorrect. In the absence of ZFS, Equations (15) and (19) become equivalent to the expression for doublet states derived previously by Moon and Patchkovskii [8]. In our notation with Z_{kl}, this corresponds to

$$Z_{kl} = \frac{S(S+1)}{3}\delta_{kl} \quad \text{[no ZFS]} \tag{20}$$

(δ_{kl} is the Kronecker delta). In this case, the pNMR shielding represents the Curie term for one of the states λ in Equation (10):

$$\boldsymbol{\sigma}^{\text{pNMR}}_{\text{Curie}} = -\frac{\beta_e}{g_N \beta_P}\frac{S(S+1)}{3k_B T}\mathbf{g}\,\mathbf{A}^N \tag{21}$$

S does not need to be a pure electron spin. When spin-orbit coupling is significantly strong, e.g. in comparison to the energy gap between the ground state and the first excited state, then spin ceases to be a good quantum number. As in EPR spectroscopy, S is then the pseudo-spin (fictitious spin) chosen to match the $2S+1$-fold degeneracy of the multiplet.

The pNMR shift is traditionally considered to arise from two main separate contributions, the *contact* (c) term, and *pseudo-contact* (pc) term. In a *nonrelativistic* framework with point nuclei, the HyF coupling matrix has an isotropic 'Fermi contact' contribution given by the expectation value

$$A^{\text{FC}}_{ij} = \frac{g_e \beta_e g_N \beta_P}{\langle S_z\rangle}\frac{\mu_0}{4\pi}\frac{8\pi}{3}\delta_{ij}\left\langle \delta(\boldsymbol{r}_N)\hat{S}_z\right\rangle \tag{22a}$$

and an anisotropic (traceless) dipolar (spin-dipole, or SD) contribution

$$A^{\text{SD}}_{ij} = \frac{g_e \beta_e g_N \beta_P}{\langle S_z\rangle}\frac{\mu_0}{4\pi}\left\langle \left(3\frac{r_{Ni}r_{Nj}}{r_N^5} - \frac{\delta_{ij}}{r_N^3}\right)\hat{S}_z\right\rangle \tag{22b}$$

Here, $\boldsymbol{r}_N$ is the electron-nucleus distance vector, r_N its length, and r_{Nu} one of its components, and g_e is the free electron g-value ($g_e \simeq 2$). The FC term probes the spin density *at* the nucleus, via the Dirac delta distribution $\delta(\boldsymbol{r}_N)$, hence the reference to 'contact'. In the pNMR shift expression (21), it is multiplied with the isotropic part of $\mathbf{g}$ and this defines the contact shielding. If $\mathbf{g}$ also has an anisotropic component, then the anisotropic dipolar part of the HyF matrix can also contribute to the isotropic chemical shift. This is the origin of the pc (dipolar) pNMR shift. In a

relativistic quantum theoretical framework, the distinction becomes blurred and the operators are different. For instance, SO coupling may generate isotropic contributions in the SD mechanism and anisotropic components in the FC mechanism. As a working definition [17], we refer to pc or dipolar shifts as the contribution arising in Equation (21) from the anisotropic part of the HyF coupling matrix. Contact shielding is associated with the isotropic component of the HyF matrix. A similar distinction has also been proposed in Reference 27. The distinction between contact and dipolar terms remains somewhat intact in relativistic calculations of HyF coupling on heavy element compounds except for the most extreme cases of SO coupling [28, 29]. There is a third contribution to the nonrelativistic one-electron HyF Hamiltonian, which is often referred to as the paramagnetic spin – orbital interaction (PSO, between the nuclear spin and the electron orbital angular momentum):

$$\hat{h}^{\mathrm{PSO}} = \frac{e}{m_e}\frac{\mu_0}{4\pi}\boldsymbol{\mu}_N \cdot \left(\frac{\boldsymbol{r}_N}{r_N^3} \times \hat{\boldsymbol{p}}\right) \tag{22c}$$

In the absence of orbital degeneracies and SO coupling, the PSO mechanism does not contribute to the HyF coupling. However, for systems where SO coupling is strong or orbital angular momentum contributions arise locally around atom N, then the PSO mechanism can become very important. The PSO operator is also central to the Ramsey shielding because it has a non-vanishing cross term with the Zeeman operator in the LR term that is typically responsible for most of the observed chemical shifts of light-atomic diamagnetic systems.

The partitioning of the pNMR shielding into contact, dipolar, and PSO contributions is not unique to the EPR parameter-based formulation because different contributions to the HyF operator in the SvH shielding expression in Equation (4) can be defined in the same way. In a relativistic framework, as already mentioned, the distinction between spin and orbital angular momenta blurs but in two-component relativistic formalisms it is usually straightforward to identify the relativistic analogs of FC, SD, and PSO.

Another approximate pNMR expression for ligand chemical shifts in metal complexes is potentially useful when metal - ligand covalency is weak or absent. In this case, there is little or no spin density that 'leaks' from the paramagnetic center to the ligand, and contact shifts are small or vanish altogether. The anisotropic term in the HyF operator then plays a decisive role. The electronic magnetic moment can be calculated via the susceptibility tensor $\boldsymbol{\chi}$ while for the HyF interaction in Equation (22b) the spatial distribution of the magnetization is ignored and approximated by a point magnetic moment at the metal center. The approach has been discussed in detail by Bertini et al. [30, 31], who also provided several equivalent variants of the resulting expression

for the pc shift. Among them, the most general expression reads

$$\delta_{\mathrm{pc}}^{\mathrm{pNMR}} = \frac{1}{12\pi r^5} \mathrm{tr}\left[\left(3\boldsymbol{r}\otimes\boldsymbol{r}^T - r^2\right)\boldsymbol{\chi}\right] \tag{23}$$

Here, $\boldsymbol{r}$ is the vector from the paramagnetic center to the NMR nucleus of interest, r its length, and $\otimes$ indicates the outer product of a column vector and a row vector (indicated by ^{T} for a transpose) to form a 3×3 matrix. Note that

$$\frac{1}{r^5}\left(3\boldsymbol{r}\otimes\boldsymbol{r}^T - r^2\right)_{ij} = 3\frac{r_i r_j}{r^5} - \frac{\delta_{ij}}{r^3} \tag{24}$$

A non-zero pc shift requires magnetic anisotropy. The T-dependence of the pc shift is absorbed into the susceptibility. Bertini gave the principal components of the susceptibility tensor for a specific multiplet, absent magnetic coupling to other states, in terms of the corresponding EPR g-factors as

$$\chi_i = \mu_0\beta_e^2 g_i^2 \frac{S(S+1)}{3kT} \tag{25}$$

Using (25) in (23) leads to an expression for the dipolar shielding that resembles Equation (21) if in the latter the HyF coupling matrix is approximated by using a point magnetic moment at the metal center [32]. We note in passing a recent article [33] suggesting a formalism to calculate from observed pc shifts back to the Hessian (second derivative matrix as a function of position) of a spatial function. The nonrelativistic form of the SD operator as in Equation (22b) shows that spatial density information recovered from pc shifts or HyF couplings should be the spin density, or more generally the magnetization density which gives rise to the susceptibility.

Observed pNMR shifts do not always exhibit a $1/T$ dependence on temperature. For instance, Bleaney [3] derived an Equation similar to (23) using CF theory in order to explain a $1/T^2$ temperature dependence of ligand NMR shifts that had been observed for certain lanthanide complexes. In this case, a weak CF splits the components of the ion's ground state term such that the energy gaps are small compared to $k_B T$, and the different states are all thermally populated (high temperature limit). The magnetic anisotropy then averages to zero in the leading $1/T$ term and only contributes to the pc shift in order $1/T^2$. Contact shifts always have a leading order of $1/T$. In the case of lanthanide complexes, it is often assumed that ligand contact shifts do not arise because of the lack of $4f$ covalency. The different T-dependence in the high-temperature limit has been used occasionally to separate contact and pc shifts in experimental studies, via variable temperature (VT) NMR measurements and fitting the data to inverse powers of T. Further details are provided in Section 3.

We recently discussed similar scenarios in which the EPR parameter-based formulation of the SvH shielding expression, Equation (14), would lead to a vanishing contribution in order $1/T$ but

non-zero in order $1/T^2$ for the pc shifts of a spin multiplet subject to ZFS [17]. The condition is that the g-tensor anisotropy Δg vanishes while ZFS is appreciable. For these cases, we also showed that the contact shift contribution of order $1/T^2$ vanishes. Alternatively, one may have a situation similar to the one considered by Bleaney where there is a set of multiplet components very close in energy such that the high-T limit applies, and among which Δg averages to zero. In this case, the leading order of the temperature-dependence of contact and pc shifts may also be $1/T$ and $1/T^2$, respectively. A separation of observed shifts into contact and pc contributions due to their different T-dependence then seems possible, as long as non-vanishing $1/T^3$ terms in both contributions are not inadvertently fit to $1/T^2$. For one of the spin multiplets investigated ($S = 3/2$) the leading order for contact and pc shifts was always $1/T$ and both had non-vanishing $1/T^2$ contributions. Due to these and other intricacies, such as the question whether the high-temperature limit is really applicable, we recommend caution when assigning contact versus pc shifts via fitting of VT data.

3 pNMR chemical shifts: Selected case studies and overview of recently published computational studies

First, selected case studies, mostly from the author's research, are discussed in order to highlight the magnitude of pNMR effects on chemical shifts, the origin of contact shifts in ligands of complexes with paramagnetic metal centers, and the dominance of the PSO mechanism on the pNMR ligand shifts of actinyl complexes. Subsequently, a brief overview of recently published studies featuring calculations of pNMR chemical shifts is provided.

Figure 1 shows calculated versus experimentally determined proton chemical shifts for the organic radical 2-methylphenyl-t-butylnitroxide (MPBN). The chemical shifts are clearly far outside of the typical proton shift range of diamagnetic compounds, with an experimental chemical shift range of over 100 ppm. pNMR calculations for MPBN were previously presented by Moon and Patchkovskii [8] as a proof-of-concept. The calculated g-factors for the molecule are very close to the free electron g-value (g_e), and therefore the pNMR effects are assigned to contact shifts which occur along with sizable isotropic proton hyperfine coupling constants. The latter are in turn caused by non-zero contact spin densities at the protons. The radical is formally described by an unpaired orbital (the 'singly occupied molecular orbital', or SOMO) that is partially conjugated with the phenyl π system. Since the phenyl π orbitals have a node the plane of the ring, the spin density at the protons is to some degree generated by the spin-polarization mechanism described by McConnell [34,35]. Figure 1 shows that the pNMR proton shifts are sensitive to the choice of the functional when DFT is used for such calculations. This is a typical finding [36,37].

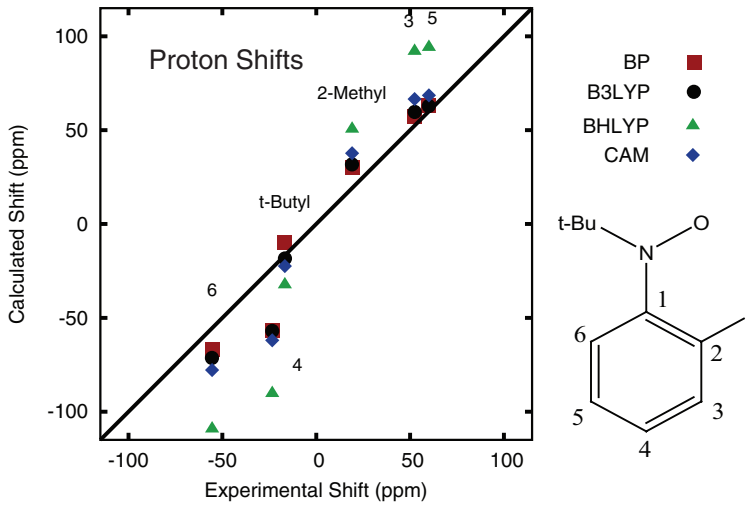

Figure 1: Calculated ^{1}H pNMR chemical shifts for the 2-methylphenyl-t-butylnitroxide radical (MPBN). The shifts are based on Equations (9) and (21), with **g** and **A** obtained from spin-unrestricted scalar relativistic DFT calculations with different functionals as indicated in the plot legend. CAM is short for CAMB3LYP. See Reference 29 for details.

In Reference 29, we also showed that the proton shifts of MPBN are sensitive to the functional used for optimizing the structure of the molecule because it influences the torsion angle of the tBu−N−O group relative to phenyl which in turn impacts the extent of π-conjugation between these moieties.

Le Guennic et al. [38] reported the synthesis, experimental characterization, and theoretical study of several diamagnetic Ru(bis-phosphine)(bis-semi-quinone) complexes. The measured ligand proton NMR spectra exhibited a pronounced temperature-dependence of the proton shifts, with some of them changing by as much as 1 ppm between 260 and 325 K. Conformational changes were ruled out as a source of the temperature dependence. Instead, DFT calculations indicated that these complexes, while having closed-shell singlet ground states, also afford very low triplet excited states. The geometry-optimized triplets were found to be only between 0.13 and 0.17 eV (1.1 to 1.4 times 10^3 cm^{-1}, or 13 to 16 kJ/mol, depending on the ligand) above the optimized singlets. With the singlet-triplet energy gap $\Delta E_{ST} = E_T - E_S$, thermal population of the triplet would give observed Boltzmann-averaged chemical shifts

$$\delta = \delta_{\text{singlet}} + 10^6 \frac{g_e \beta_e}{g_N \beta_P} \frac{S(S+1)}{k_B T} A^N \left(3 + e^{\Delta E_{ST}/(k_B T)}\right)^{-1} \tag{26}$$

The $1/T$ dependence of the Curie pNMR contact shift in the excited state is counter-balanced by an increasing population of the excited state with increasing temperature. Values for ΔE_{ST} and the isotropic hyperfine coupling constants A^N extracted from fits of the experimental variable-

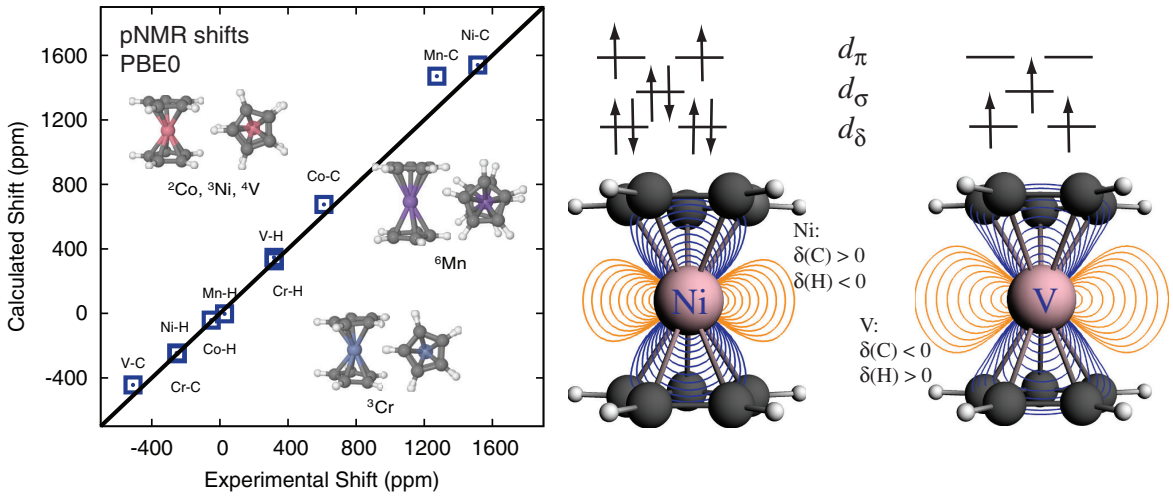

Figure 2: Left: Calculated ^{13}C and ^{1}H pNMR shielding for the Cp ligands of different 3d metallocenes, using Equation (21) with **g** and **A** obtained from scalar relativistic DFT calculations. The effects of ZFS were neglected. $T = 298$ K (389 K for Mn). The spin multiplicities are written as superscripts in front of the metal's chemical symbols. See Reference 29 for details. Right: Formal occupations of the Ni and V 3d orbitals of nickelocene and vanadocene, respectively, and contour line plots of the $3d_\sigma$ orbitals. The energetic ordering of d_σ and d_δ may vary, depending on the functional used.

temperature (VT) data to Equation (26) were in good agreement with the calculated ΔE_{ST} and A^N.

In 2007, Hrobarik et al. [25] provided an important proof-of-concept that DFT calculations via the EPR parameter route are able to describe pNMR chemical shifts for states with arbitrary spin-multiplicity. Calculations were performed for the series of open-shell 3d metallocenes, MCp_2, with M = V, Cr, Mn, Co, Ni and Cp = C_5H_5. Given the large experimental C and H ligand chemical shift ranges for these complexes, the agreement of the calculations with experimental data was good. Hrobarik et al. also proposed a treatment of ZFS in such calculations but found that its effects on the isotropic shifts was small or negligible. Our group subsequently performed calculations on these metallocenes with our own implementation for EPR hyperfine and Zeeman coupling in which scalar relativistic effects were treated variationally and SO effects were included as a perturbation [29]. The comparison of calculated versus experimental ligand carbon and proton NMR shifts of open-shell MCp_2 complexes is shown in the left hand side panel of Figure 2. The calculations indeed reproduce the signs and magnitudes of the large pNMR effects quite well. It is important to note that 150 ppm deviation from experiment for a calculated carbon shift or several dozen ppm for a proton would be completely unacceptable for diamagnetic systems. Due to the large pNMR chemical shift ranges, however, the error bars of the calculations on paramagnetic compounds are amplified as well.

Reference 29 addressed the origin of the pNMR effects on the ligand chemical shifts. For example, $NiCp_2$ (nickelocene) has a spin-triplet ground state with two unpaired electrons. The carbon shifts are very large and positive, while the proton shifts are negative. VCp_2 (vanadocene) has a quartet ground state and affords negative carbon shifts and positive proton shifts. Even though vanadocene has one more unpaired electron as nickeleocene, the pNMR effects on the carbon shifts are much smaller in magnitude. (However, together with $CrCp_2$, vanadocene affords the largest proton shifts among the samples.) For these and the other metallocenes, the pNMR effects are dominated by contact shifts which, per Equation (21), are proportional to the isotropic HyF coupling constants. A per-orbital analysis of the HyF coupling in terms of localized molecular orbitals (LMOs) was developed to dissect the results. The LMO data for VCp_2 and NiCp2 are collected in Table 1. Qualitative orbital diagrams for the $3d$ orbitals of the complexes are shown in the right hand side panel of Figure 2, together with contour line plots of the $3d_\sigma$ orbitals.

The proposed mechanism responsible for the pNMR shifts of $NiCp_2$ has an interesting history. In 1957, McConnell and Holm observed an 'unusual' proton nuclear resonance shift for nickelocene [39], with the sign of the shift being unusual because it implied negative (β-) spin density at the protons for the $M_S = 1$ component of the triplet. Pseudo-contact shifts were ruled out. The sign was explained by noting that 'unpaired spins move off the nickel atom and onto the aromatic cyclopentadienyl rings', with '$\sigma - \pi$ configuration interaction' (i.e. spin polarization) producing

Table 1: Localized molecular orbital decomposition of the isotropic ^{13}C HyF coupling constants of vanadocene (spin quartet) and nickelocene (spin triplet), in MHz[a]. The isotropic ^{13}C pNMR shifts are overwhelmingly caused by the contact term, which is proportional to the HyF constant. See the text and Reference 29 for details.

orbital type	V	Ni
C (core)	-1.92	0.23
σ bonds (NN)	0.89	2.40
other σ bonding/core, same Cp	-0.64	0.98
π bonds, same Cp	-0.24	0.16
other σ bonding/core, other Cp	0.02	-0.01
π bonds, other Cp	0.03	0.47
Metal (core)	-0.02	-0.01
Metal d_σ	*0.74	0.02
Metal d_π		*0.85
Metal d_δ	*0.07	-0.03
total	-1.06	5.06

[a] Scalar relativistic DFT calculations (PBE0 functional). NN = nearest neighbor atoms to the carbon for which the HyF coupling constant was calculated. The unpaired metal orbitals are indicated by *. The symmetry classification of the metal d orbitals is with respect to the principal symmetry axis of MCp_2. See also the right panel of Figure 2.

unpaired spin density at the protons of opposite sign than the overall value of $\langle S_z \rangle$. The spin-polarization effect is general and explains the opposite signs of the C and H shifts found for most of the metallocenes seen in Figure 2. For nickelocene, the 1957 McConnell and Holm interpretation of the proton shift implies positive spin density and positive HyF coupling at the carbons. In 1958, upon observation of proton NMR shifts for vanadocene and chromocene of opposite sign than for $NiCp_2$, McConnell and Holm postulated a different mechanism for nickelocene, namely 'charge transfer bonding between the nickel ion and the carbon atoms. [...C]harge having a spin polarization opposite to that of the spin on the Ni++ ion is transferred from the rings to the central ion. This leaves a positive spin density on the carbon atoms that in turn produces a negative spin density at the protons.' [40] In other words, the mechanism proposed in 1958 was selective β-spin ligand $\rightarrow$ metal dative bonding, leaving a net α-spin density at the carbons. The outcome is the same as for the mechanism proposed a year earlier, but which one is the right explanation?

Refer to Table 1 for the nickelocene ^{13}C HyF coupling analysis. There is a direct contribution from the unpaired Ni $3d_\pi$ orbitals which amounts to 17% of the total isotropic HyF coupling, with the same sign. This can be interpreted as the contribution from the 1957 McConnell and Holm mechanism where 'unpaired spins move off the nickel atom [...]'. Clearly, the ligand cannot donate electron density to the Ni α-spin $3d$ orbitals because they are all occupied (Figure 2). However, the formally unoccupied Nickel β-spin $3d_\pi$ orbitals were calculated to have populations of 0.4 electrons each, which clearly reveals the selective β-spin ligand $\rightarrow$ metal dative bonding. The Cp π orbitals do not give large contributions in the analysis because the isotropic HyF coupling requires a contact spin density, which is generated via spin polarization and shows up in form of contributions from the Cp σ orbitals. (In reference to the Cp orbitals, the labels σ and π in Table 1 have their usual organic chemistry meaning. The Cp orbitals donating to Ni may be classified as $\pi_{Cp}\pi_{\|}$, with $\|$ indicating the symmetry with respect to the principal symmetry axis of MCp_2.) In conclusion, McConnell and Holm were 17% right in 1957 and 83% right in 1958.

The negative ^{13}C HyF coupling in vanadocene has a different explanation. The unpaired α-spin $3d_\sigma$ orbital is spatially much more extended than the corresponding Ni orbital (Figure 2) and therefore it can overlap better with the carbon core orbitals. This explains the large positive contribution from this orbital to the total HyF coupling. Due to Pauli exclusion, however, the carbon core orbitals and some Cp σ orbitals are strongly spin-polarized in the opposite direction. The latter effect ends up dominating the result and the HyF coupling constants are negative. Selective donation of β spin-density from the ligands to the metal is not very effective in vanadocene because there are no occupied $\pi_{Cp}\delta_{\|}$ ligand orbitals and donation from $\pi_{Cp}\sigma_{\|}$ is energetically less favorable.

In Reference 41, the role of spin in ligand $\rightarrow$ metal dative bonds and its impact on ligand pNMR shifts was investigated in more detail. The study emphasized the role of the DFT delocal-

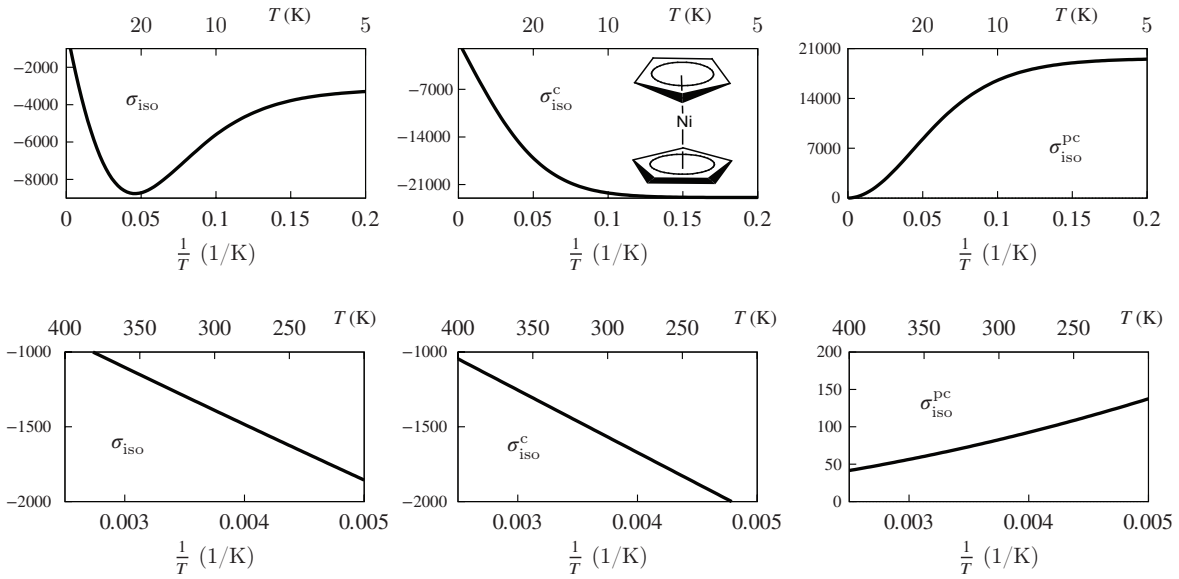

Figure 3: Calculated isotropic ^{13}C pNMR shielding for the Cp ligands of nickelocene, $NiCp_2$, in its spin-triplet ground state as a function of T. From left to right: Total shielding, contact, and dipolar (pc) contribution. Data based on Equation (14), using **g** and **A** from scalar relativistic DFT calculations (PBE0 functional) and the experimental ZFS parameter of 25.6 cm^{-1} to calculate **Z**. See Reference 17 for details.

ization error [42], which tends to exaggerate the covalency in ligand - metal bonds in calculations with functionals that afford no or small fractions of exact exchange. A series of metal tris-acac complexes was chosen for the study; these complexes were previously also investigated by Rastrelli and Bagno [43, 44]. The isotropic ligand HyF coupling constants and pNMR shifts indeed showed that their magnitude is well correlated with the extent to which DFT calculations tend to overestimate the covalency of the ligand - metal bonds. The signs of the pNMR shifts in the tris-acac complexes can be rationalized by considering dative ligand → metal bonding that is selectively stronger for one of the spin projections, not unlike the case of nickelocene where α-spin ligand → metal donation is absent because of the filled $3d$ α-spin shell. Whenever such dative bonding with imbalanced spin contributions is possible it has a potential for creating spin density in the ligands.

The effects of ZFS on the ^{13}C pNMR shielding constants of nickelocene based on the EPR parameter version of the SvH formalism, Equation (14), were studied in Reference 17. The bottom row panels of Figure 3 show the temperature dependence between 200 and 400 K, the top row shows the behavior for very low temperatures. Since the complex affords a negligible g-tensor anisotropy for the spin triplet, the dipolar (pseudo-contact, pc) shielding in the right column arises only because of the sizable ZFS. At higher temperatures, the plots exhibit the expected linear behavior as a function of $1/T$ for the contact shielding and a non-linear behavior for the dipolar

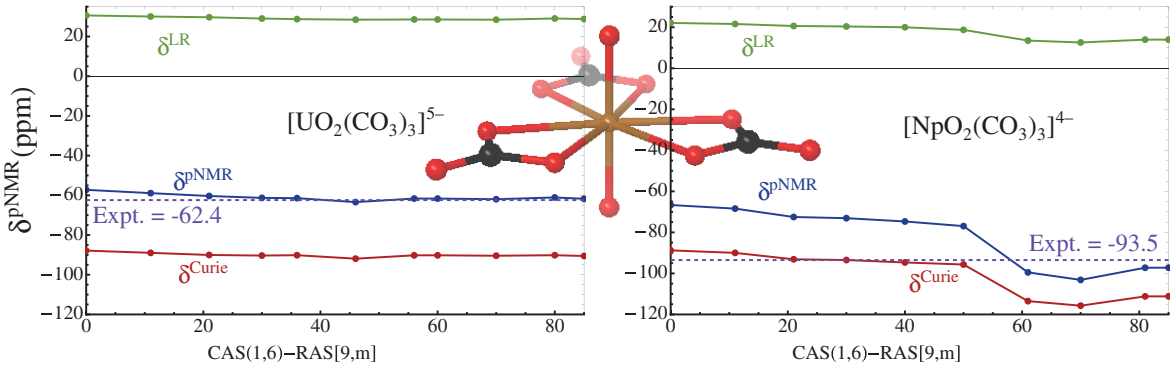

Figure 4: Calculated ^{13}C ligand pNMR chemical shifts for two $5f^1$ actinyl tris-carbonate complexes. The shift reference is an isostructural diamagnetic U^{VI} complex. Multi-reference wavefunction calculations including scalar and SO relativistic effects were used to calculate the shifts per Equation (10). The abscissas indicate restricted active spaces used to create spin polarization. The experimental chemical shifts are also indicated. See Reference 13 for details.

Table 2: Breakdown of the calculated pNMR shift Curie terms (ppm, times −1) of Equation (10) for the $E_{3/2}$ ground state and the $E_{1/2}$ excited state Kramers doublets of $[NpO_2(CO_3)_3]^{4-}$ and $[UO_2(CO_3)_3]^{5-}$ into contributions from contact (FC), dipolar (SD), and spin-orbit (PSO) mechanisms. Data corresponding to the RAS[9,85] calculations of Figure 4. The FC, SD, and PSO mechanisms contributing to the Curie terms according to the EPR parameter formulation, Equation (21), are also listed. See Reference 13 for details.

Curie	'direct', Eq. 10				EPR route, Eq. 21			
	total	FC	SD	PSO	total	FC	SD	PSO
$[NpO_2(CO_3)_3]^{4-}$								
$E_{3/2}$	109.65	22.79	28.43	58.42	109.78	22.82	28.46	58.49
$E_{1/2}$	130.06	-47.94	32.86	145.14	130.21	-47.99	34.54	144.21
$[UO_2(CO_3)_3]^{5-}$								
$E_{3/2}$	82.71	3.39	25.30	54.01	82.80	3.39	25.33	54.07
$E_{1/2}$	113.05	-60.70	33.10	140.65	113.18	-60.77	34.88	139.82

shielding, which corresponds to the high-temperature limit for the elements of the matrix $\mathbf{Z}$ in Equation (15). At ambient temperatures, the dipolar shielding is overall small and can be ignored when interpreting the NMR spectrum. Evidently, at low temperatures the T-dependence of the shielding becomes more intricate, with a T-dependent balance of negative contact and positive dipolar contributions of comparable magnitude.

Our group recently reported direct calculations of pNMR chemical shifts of paramagnetic metal complexes, using Equation (10) instead of an EPR parameter-based formalism [13]. The direct approach became necessary for a rather challenging application scenario with orbital degeneracies, the presence of very low electronic excited states, and strong spin-orbit (SO) coupling,

namely pNMR ligand shifts of actinide complexes. Experimental isotropic ^{13}C NMR solution data are available, for instance, for $[UO_2(CO_3)_3]^{5-}$ (U(V)) and $[NpO_2(CO_3)_3]^{4-}$ (Np(VI)) [45,46]. Both complexes exhibit sizable ^{13}C pNMR shifts relative to the isostructural diamagnetic U(VI) complex $[UO_2(CO_3)_3]^{4-}$. The chemical shifts of the paramagnetic systems are also surprisingly different given that the U(V) and Np(VI) complexes are isostructural and isoelectronic. We determined previously that DFT calculations of the magnetic properties of such open-shell actinide complexes are possible but fraught with issues [47,48]. Therefore, the calculation of the required integrals in Equation (10) was implemented within a complete active space and restricted active space self consistent field (CASSCF, RASSCF) multi-reference wavefunction framework [49]. Starting with a principal active space that includes the $5f$ orbitals of the metal, the RAS paradigm was used to generate additional spin polarization and contact spin density at the carbon nuclei in the ligands (without re-optimizing the CAS orbitals). Figure 4 shows the convergence of the calculated shift and the Curie and LR contributions arising from the open metal shell with respect to the size of the active space (these are Boltzmann averages over the two lowest-energy Kramers doublets). The experimental pNMR shift is also indicated. The calculations converge to a nearly quantitative agreement with experiment and also reproduce the difference of the ^{13}C shift between the U(V) and Np(VI) complex.

The matrix elements of $\hat{H}_{Ni}^{\mathrm{HyF}}$ are critical for the pNMR shielding. As pointed out in Section 2, the HyF interaction is determined by three mechanisms [18,50]: Fermi-contact (FC), spin-dipole (SD), and paramagnetic spin - orbital (PSO). In the absence of SO coupling and (local) orbital angular momentum, PSO does not contribute to the HyF coupling and the pNMR shift and it is therefore often ignored. However, for the two actinide complexes, the PSO mechanism is critical. A breakdown of the Curie terms for the two lowest electronic states in terms of these mechanisms is given in Table 2. The Curie terms were also calculated from EPR parameters determined from the same wavefunctions, and the breakdown per mechanism is likewise listed in the table. The PSO mechanism is the dominant one in all cases. However, the contact and dipolar mechanisms are also important, and they may reinforce or cancel each other. Moreover, for a given multiplet, the Curie term of the 'direct' calculation agrees very well with the EPR parameter-based variant. There is presently not a large enough body of data available in order to know whether this is generally the case or not, but the agreement is encouraging.

The Boltzmann average of the Curie shifts generated by each multiplet corresponds to δ^{Curie} in Figure 4 and represents the dominant contribution to the carbon pNMR shifts of these actinyl complexes. Magnetic coupling between the low-energy electronic states produces a Boltzmann average of the LR contributions that are of opposite sign to the Curie contributions, but smaller in magnitude. The two doublets are separated by 142 (U) and 356 (Np) cm^{-1}, respectively, which helps to rationalize the larger magnitude of the LR contribution in the uranyl complex. The com-

bination of the LR difference with the sizable contact shift in the ground state of the neptunyl complex is seen to be responsible for the different chemical shifts of these two isostructural and formally isoelectronic paramagnetic complexes.

Recently published articles on the topic demonstrate that there is on-going interest in calculating and analyzing the effects of electron paramagnetism on NMR parameters. Often, results from such computations are published in joint theoretical-experimental studies. For instance, Szalontai et al. [51] employed Equation (22a) with DFT calculations to determine ^{13}C and ^{2}H contact shifts of several copper(II) complexes containing amino acids and carboxylic acids and compared them to experimental magic angle spinning (MAS) solid-state NMR spectra. The study demonstrated the ability to differentiate between *D*, *L* and *L*, *L* diastereomers of alaninato complexes. The authors also showed that the three-bond HyF coupling has a Karplus-like dependence on the torsional angles, which turned out to be helpful with the assignment.

Kong et al. [52] used DFT and Equation (22a) to calculate ^{17}O chemical shifts of six complexes containing first row transition metals, namely $V(acac)_3$, $K_3V(Ox)_3 \cdot 3\,H_2O$, $Cu(DL-Ala)_2 \cdot H_2O$, $K_2Cu(Ox)_2 \cdot 2\,H_2O$, $Mn(acac)_3$, and $Cu_3(BTC)_2(H_2O)_3$ (BTC = benzenetricarboxylate), with an observed (MAS) chemical shift range of over 10,000 ppm. The authors assumed an isotropic free-electron *g*-tensor and consequently ignored the dipolar shifts. A variety of functionals was tested, with the LC-ωPBE functional performing the best when compared to experiment. DFT was shown to give reasonable agreement with experiment over the 10,000 ppm shift range. Some discrepancies were noted for directly chelating oxygens, which was attributed to possibly being caused by some of the neglected contributions, i.e. dipolar shifts, bulk magnetic susceptibility, ZFS, by inaccuracies in the crystal structures, crystal packing effects, by approximations in the electronic structure model, and in the case of $Mn(acac)_3$ by large uncertainties in the experimental shifts. The role of preferential α- or β-spin ligand $\rightarrow$ metal donation noted previously in References 29 and 41 was emphasized.

Cheng et al. [53] utilized DFT calculations and variants of Equations (22a), (23), and (25) to estimate dipolar contributions to ^{13}C and ^{1}H shifts of an $S = 1$ $Ni^{III}(OETPP^{\cdot})Br_2$ radical complex (OETPP = dianion of 2,3,7,8,12,13,17,18- octaethyl-5,10,15,20-tetraphenyl-porphyrin) representing a model for Factor 430, a cofactor of methyl coenzyme reductase. The studied complex was the first example of a porphyrin radical comples for which structural and pNMR data became available. The observed pNMR shifts were assigned as predominantly of contact nature. In the article's supplementary information, it was stated that contact shifts obtained with DFT are systematically overestimated due to the contact spin density being calculated at the exact center of the nucleus versus within a sphere containing the center of the nucleus, although the magnitudes of the contact spin densities correlated rather well with the chemical shifts. The claim was not further substantiated and appears to be a result of identifying systematic errors in the contact shift

calculations with those of calculations of Mössbauer isomer shifts. While it is true that the contact operator in Equation (22a) is the nonrelativistic version corresponding to a point magnetic nuclear dipole moment, it should be a suitable approximation for the hyperfine operator of light ligand atoms such as the ones studied by Chen et al. The noted systematic errors in the DFT calculations of the contact shifts likely have other reasons.

Rouf, Mares, and Vaara [54] used a combination of DFT and CASSCF to calculate ^{1}H shifts of three cobalt^{II} pyrazolylborate complexes using the EPR parameter route. The spin Hamiltonian parameters were calculated with DFT, and **g** and **D** were also calculated using CASSCF and CASSCF with N-electron valence state perturbation theory to second order (NEVPT2) to treat dynamic correlation. Much larger values were calculated with the wavefunction methods, but experimental data were not available for comparison. After reassigning one of the proton positions, the DFT/NEVPT2 calculations gave very good agreement with experimental proton chemical shifts.

Mares et al. [55] utilized the EPR parameter-based approach to calculate ^{17}O and ^{1}H paramagnetic shifts of solvent waters from snapshots of a molecular dynamics (MD) trajectory of an aqueous Ni^{2+} ion. The MD simulation employed a polarizable force field. **A** and **g** were calculated with DFT, and NEVPT2 was used for the ZFS matrix **D**. The purpose of the study was to determine the contributions to the relaxation rates from the paramagnetic (Curie-type) mechanism. The contributions of Curie relaxation for both nuclei were found to be negligible at currently used MRI field strengths, despite the presence of large hyperfine shifts in particular in the first solvation shell around the nickel ion. See also a 2011 article by Mares et al. on paramagnetic shifts in solvent molecules around Ni^{2+} [56].

Fusaro, Casella, and Bagno [57] performed NMR measurements along with DFT calculations of ^{17}O contact shifts for the MRI contrast agent Gd(DOTA)$^{-}$ (DOTA=tetraazacyclododecanetetraacetic acid). The calculations utilized the EPR parameter-based formalism. Due to the Gd^{3+} ion having an isotropic magnetic susceptibility tensor, dipolar shifts were neglected. The calculations included scalar relativistic effects variationally, and SO effects on the g-factors and HyF coupling tensors via perturbation theory. The calculations also provided estimates of the relaxation rates due to different relaxation pathways such as the quadrupolar interaction and paramagnetic broadening. The main conclusion was that carbonyl oxygens in DOTA are directly detectable by NMR due to the lack of paramagnetic broadening, which may stimulate further NMR characterization of small Gd^{3+} complexes that are potentially useful as contrast agents.

Borgogno, Rastrelli, and Bagno [58] calculated the relative energies of different spin states with DFT for a set of 16 paramagnetic iron complexes with a wide variety of organic ligands, within the context of spin crossover. Some of the porphyrin-containing complexes had assigned experimental NMR specta. EPR parameter-based calculations of ^{1}H shifts were performed for

these complexes and the simulated spectra for different spin states were compared with the experimental data. The authors concluded that the relative energies calculated with the B3LYP functional ranked the spin states reliably. Moreover, the agreement of calculated and experimental pNMR shifts were deemed to be good enough in order to allow for a reliable assignment of the spin state responsible for the observed experimental NMR data.

In Reference 27, Komorovsky et al. compared EPR parameter-based four-component relativistic DFT calculations of ligand pNMR shifts for two Ru(III) complexes with two earlier studies by other groups where the two-component zeroth-order regular approximation (ZORA) had been used to treat relativistic effects [32,44]. The authors came to a contrary conclusion to that of Rastrelli and Bagno [44] in that they deemed fully relativistic calculations necessary for these complexes because there were noticeable differences between the four-component and ZORA HyF couplings. However, there were numerous technical differences between the calculations, other than the level at which relativistic effects were treated. It is therefore possible that other reasons are responsible for the differences between the calculated data.

In a joint experimental - computational study, Rudolph et al. [59] utilized the EPR parameter-based approach to calculate proton pNMR shifts for a Fe, Ni, S complex with a mono-radical $Ni-\mu-S_2-Fe$ core that is reminiscent of the active site of [NiFe] hydrogenase. A combination of codes was used to calculate the NMR parameters with DFT at different levels of treating relativistic effects. The calculations were used to help assigning the experimental shifts. The best computational results were obtained with a modified B3LYP functional with 10% exact exchange. The same functional was also used to calculate ^{57}Fe Mössbauer parameters, viz. nuclear quadrupole coupling and the isomer shift.

In the Introduction it is mentioned that the CF theory based approach is still in use, and Section 2 alludes to the different T-dependence that can be attributed to contact and dipolar shifts under certain conditions, chiefly among them the validity of the high-T limit or lack of g-tensor anisotropy. The high-temperature limit is expected to apply to lanthanide complexes where the CF interaction with the open $4f$ shell tends to be weak, but it is much less likely to apply to transition metal and actinide complexes where the ligand-induced splitting of the metal ion's ground state multiplet components is much larger. An example where results from VT measurements were used to assign the nature of ligand shifts in lanthanide complexes is Reference 60. Walton et al. measured and analyzed solution NMR data of lanthanide complexes with a nonadentate macrocycle ligand based on triazacyclononane. The observed linear variation of the methylene proton shifts as $1/T^2$ was argued to indicate the dominance of the dipolar mechanism. An example where VT NMR data were explicitly fit to $1/T$ versus $1/T^2$ is Reference 61. Yamada et al. synthesized adducts of C_{80} cage containing two lanthanum or cerium ions with an adamantylidene. ^{13}C NMR spectra were obtained for the cerium containing complex at various temperatures and the data

was plotted against $1/T$ and $1/T^2$, respectively. Only the $1/T^2$ fit was reasonable, leading to an assignment as dominantly dipolar based on the analysis put forward by Bleaney. In a similar fashion, ^{13}C spNMR shifts if $[CeC_{82}]^-$ and ^{45}Sc pNMR shifts of $[CeSc_2NC_{80}]$ were assigned as dipolar [62, 63].

Instead of fitting observed VT NMR data, there is another way by which contact and pc shifts are commonly separated if there are experimental data for a series of related lanthanide (Ln) compounds available. This is sometimes referred to as the Reilley method [64], which was critically reviewed by Di Pietro, Piano, and Di Bari in 2011 [65]. Based on the theoretical methods of Bleaney et al. and Golding et al., the isotropic shift of a ligand L in a lanthanide metal M complex with a principal axis of symmetry can be expressed as [64]

$$\delta^{\mathrm{pNMR}} = \delta^{\mathrm{cont.}}_{ML} + \delta^{\mathrm{pc}}_{ML} \tag{27a}$$

with the contact shift written as

$$\delta^{\mathrm{cont.}}_{ML} = \langle S_z \rangle_M F_L \tag{27b}$$

and the dipolar (pc) shift as

$$\delta^{\mathrm{pc}}_{ML} = \frac{aC^D_M}{T^2}\left(\frac{3\cos^2\theta - 1}{r^3}\right) = C^D_M G_L \tag{27c}$$

for an axial system. In Equation (27b), $\langle S_z \rangle_M$ is the Boltzmann-averaged spin-z magnetic moment expectation value for the metal ion's ground-state term split by the CF. It is assumed to be a function only of the metal and its electronic configuration, and it is proportional to $1/T$. Further, the contact shift expression contains a factor that is supposed to depend on the ligand atom and its position, but not on the metal. One may think of the ligand-dependent term F_L in the product $\langle S_z \rangle_M F_L$ as a contact spin-density polarizability of a specific ligand atom in a given ligand, such that when it is multiplied with the value $\langle S_z \rangle_M$ generated by the metal ion then one obtains the actual contact shift. F_L is proportional to the HyF coupling and assumed to be constant among a series of isostructural complexes with different metals. In Equation (27c), r is the distance of the ligand nucleus from the paramagnetic center, and θ is the angle between the metal-ligand distance vector and the principal axis of symmetry of the complex. The geometric factor in Equation (27c) represents the $i = j = z$ case in Equation (24) since $z = r\cos\theta$, and it corresponds to Equation (23) with an axially symmetric susceptibility tensor. The constant a depends on the crystal field, and the parameter C^D_M is a metal-dependent constant that is related to the susceptibility and its

anisotropy, as the comparison of Equation (27c) with (23) indicates. It follows that

$$\frac{\delta^{\mathrm{pNMR}}}{C_M^D} = \frac{\langle S_z \rangle_M}{C_M^D} F_L + G_L \tag{28}$$

C_M^D and $\langle S_z \rangle_M$ for different lanthanides have been tabulated. The F_L values can be extracted from the slope of a plot of the left hand side of Equation (28) for isostructural complexes with different lanthanides M. Often, this is followed by an assignment of contact and dipolar shifts for different ligands in a given complex by calculating the geometric factor in Equation (27c) from crystal structure data or from optimized structures.

Castro et al. [66] recently used a Reilley analysis to determine the relative contributions of contact versus dipolar contributions to the pNMR ligand shifts of lanthanide(III) complexes with the TPPTAM macrocycle ligand (TPPTAM = 2,2',2"-(3,7,11-triaza-1,5,9(2,6)-tr-pyridinacyclododecaphane-3,7,11-triyl)triacetamide). According to the analysis, both mechanisms give comparable contributions to the observed shifts for some of the complexes, meaning that the extent of transfer of spin density from the open $4f$ shell to the ligand would be surprisingly large. An excellent correlation of calculated dipolar shifts with the geometrical factor $(3\cos^2\theta - 1)/r^3$ obtained from DFT optimizations was used to argue that the calculations provided good models for the structures of the complexes in solution structures and that these structures are similar to those determined experimentally for the solid state.

In 2014 Martel et al. [67] performed the first high-resolution ^{17}O solid-state MAS NMR measurements on a series of highly radioactive actinide oxides. ^{17}O chemical shifts were determined for AnO_2 with An = Th, U, Np, and Am. A CF method [68] and Golding's theory [5], i.e. Equation (27b), was employed to rationalize the observed trends for the ^{17}O shifts. Because of the cubic symmetry it was assumed that the shifts were purely of contact nature. A correlation between $\langle S_z \rangle$ values calculated from CF theory and the observed chemical shifts was expected and found for the heavier actinides. It remains to be seen if the assumptions underlying Equation (27b) are valid for AnO_2 or other actinide complexes. The authors argued that the diamagnetic ground state of ThO_2 is more complicated than just an empty $5f$ shell.

4 Summary and Outlook

In the past decade, significant progress has been made toward reliable first-principles theory based calculations of pNMR chemical shifts. The theory can be adapted also for calculations of indirect nuclear spin-spin coupling. For systems with energetically well-separated electronic states, it appears to be sufficient to focus on the Curie type terms for an electronic state of interest. Further, there is some numerical evidence, based on the two lowest energy Kramers doublets of two actinyl

complexes, that the EPR parameter based calculations of the Curie pNMR shifts can reproduce the Curie contributions of a direct calculation (Equation (4)) also in situations where spin-orbit effects are sizable and the EPR pseudo-spin is not the electron spin. Magnetic coupling between electronic states may give important contributions if the energetic separation of the electronic states is small. Calculating the effects of electron paramagnetism on NMR parameters accurately remains challenging, and progress on the theoretical front is on-going.

Acknowledgments

The author acknowledges financial support for his theoretical studies of the magnetic properties of f-element complexes from the U.S. Department of Energy, Office of Basic Energy Sciences, Heavy Element Chemistry program, under grant DE-SC0001136 (formerly DE-FG02-09ER16066). The author also wishes to thank Dr. Hélène Bolvin, Dr. Frédérick Gendron, Mr. Robert Martin, Dr. Benjamin Pritchard, and Dr. Kamal Sharkas for their contributions to the project and helpful discussions, and Mr. Robert Martin for help with this chapter.

References

[1] Ramsey, N. F., 'Magnetic shielding of nuclei in molecules', *Phys. Rev.* **1950**, *78*, 699–703.

[2] McConnell, H. M.; Chesnut, D. B., 'Theory of Isotropic Hyperfine Interactions in π-Electron Radicals', *J. Chem. Phys.* **1958**, *28*, 107–117.

[3] Bleaney, B., 'Nuclear Magnetic Resonance Shifts in Solution Due to Lanthanide Ions', *J. Mag. Res.* **1972**, *8*, 91–100.

[4] Golding, R. M.; Halton, M. P., 'A theoretical study of the ^{14}N and ^{17}O N.M.R. shifts in Lanthanide Complexes', *Aust. J. Chem.* **1972**, *25*, 2577–2581.

[5] Golding, R. M.; Pyykkö, P., 'Theory of pseudocontact NMR shifts due to lanthanide complexes', *Mol. Phys.* **1973**, *26*, 1389–1396.

[6] Kurland, R. J.; McGarvey, B. R., 'Isotropic NMR Shifts in Transition Metal Complexes: The calculation of the fermi contact and pseudocontact terms', *J. Mag. Res.* **1970**, *2*, 286–301.

[7] Rinkevicius, Z.; Vaara, J.; Telyatnyk, L.; Vahtras, O., 'Calculations of nuclear magnetic shielding in paramagnetic molecules', *J. Chem. Phys.* **2003**, *118*, 2550–2561.

[8] Moon, S.; Patchkovskii, S., 'First–principles calculations of paramagnetic NMR shifts', in Kaupp, M.; Bühl, M.; Malkin, V. G. (editors), 'Calculation of NMR and EPR Parameters. Theory and Applications', Wiley-VCH, Weinheim, **2004**, 325–338.

[9] Vaara, J., 'Chemical Shift in Paramagnetic Systems', in Contreras, R. H. (editor), 'High Resolution Nuclear Magnetic Resonance Parameters for Understanding Molecules and their Electronic Structure', Vol. 3 of *Science & Technology of Atomic, Molecular, Condensed Matter & Biological Systems*, Elsevier, Amsterdam, **2013**, 41–67.

[10] Van den Heuvel, W.; Soncini, A., 'NMR chemical shift as analytical derivative of the Helmholtz free energy', *J. Chem. Phys.* **2013**, *138*, 054113 (10 pages).

[11] Soncini, A.; Van den Heuvel, W., 'Communication: Paramagnetic NMR chemical shift in a spin state subject to zero-field splitting', *J. Chem. Phys.* **2013**, *138*, 021103 (3 pages).

[12] Van den Heuvel, W.; Soncini, A., 'NMR Chemical Shift in an Electronic State with Arbitrary Degeneracy', *Phys. Rev. Lett.* **2012**, *109*, 073001 (5 pages).

[13] Gendron, F.; Sharkas, K.; Autschbach, J., 'Calculating NMR Chemical Shifts for Paramagnetic Metal Complexes from First-Principles', *J. Phys. Chem. Lett.* **2015**, *6*, 2183–2188.

[14] Dyall, K. G.; Fægri, K. Jr., *Relativistic Quantum Chemistry*, Oxford University Press, New York, **2007**.

[15] Saue, T., 'Relativistic Hamiltonians for Chemistry: A Primer', *ChemPhysChem* **2011**, *12*, 3077–3094.

[16] Autschbach, J., 'Perspective: Relativistic Effects', *J. Chem. Phys.* **2012**, *136*, 150902 (15 pages).

[17] Martin, B.; Autschbach, J., 'Temperature dependence of contact and dipolar NMR chemical shifts in paramagnetic molecules', *J. Chem. Phys.* **2015**, *142*, 054108 (10 pages).

[18] Autschbach, J.; Ziegler, T., 'Double perturbation theory: A powerful tool in computational coordination chemistry', *Coord. Chem. Rev.* **2003**, *238/239*, 83–126.

[19] Van Vleck, J. H., *The theory of electric and magnetic susceptibility*, Oxford University Press, **1932**.

[20] Ramsey, N. F., 'Chemical Effects in Nuclear Magnetic Resonance and in Diamagnetic Susceptibility', *Phys. Rev.* **1952**, *86*, 243–246.

[21] Ramsey, N. F., 'Electron coupled interactions between nuclear spins in molecules', *Phys. Rev.* **1953**, *91*, 303–307.

[22] Ziegler, T.; Seth, M.; Krykunov, M.; Autschbach, J.; Wang, F., 'Are Charge Transfer Transitions Really too Difficult for Standard Density Functionals or are They Just a Problem for Time-Dependent Density Functional Theory Based on a Linear Response Approach?', *J. Mol. Struct. (special TDDFT issue of Theochem)* **2009**, *914*, 106–109.

[23] Ziegler, T.; Seth, M.; Krykunov, M.; Autschbach, J., 'A revised electronic hessian for approximate time–dependent density functional theory', *J. Chem. Phys.* **2008**, *129*, 184114 (9 pages).

[24] Paez Hernandez, D.; Bolvin, H., 'Magnetic properties of a fourfold degenerate state: Np^{4+} ion diluted in Cs_2 $ZrCl_6$', *J. Electron Spectrosc.* **2014**, *194*, 74–80.

[25] Hrobárik, P.; Reviakine, R.; Arbuznikov, A. V.; Malkina, O. L.; Malkin, V. G.; Köhler, F. H.; Kaupp, M., 'Density functional calculations of NMR shielding tensors for paramagnetic systems with arbitrary spin multiplicity: Validation on 3d metallocenes', *J. Chem. Phys.* **2007**, *126*, 024107 (19 pages).

[26] Pennanen, T. O.; Vaara, J., 'Nuclear Magnetic Resonance Chemical Shift in an Arbitrary Electronic Spin State', *Phys. Rev. Lett.* **2008**, *100*, 133002 (4 pages).

[27] Komorovsky, S.; Repisky, M.; Ruud, K.; Malkina, O. L.; Malkin, V. G., 'Four-Component Relativistic Density Functional Theory Calculations of NMR Shielding Tensors for Paramagnetic Systems', *J. Phys. Chem. A* **2013**, *117*, 14209–14219.

[28] Verma, P.; Autschbach, J., 'Relativistic density functional calculations of hyperfine coupling with variational versus perturbational treatment of spin-orbit coupling', *J. Chem. Theory Comput.* **2013**, *9*, 1932–1948.

[29] Aquino, F.; Pritchard, B.; Autschbach, J., 'Scalar relativistic computations and localized orbital analysis of nuclear hyperfine coupling and paramagnetic NMR chemical shifts', *J. Chem. Theory Comput.* **2012**, *8*, 598–609.

[30] Bertini, I.; Turano, P.; Vila, A. J., 'Nuclear magnetic resonance of paramagnetic metalloproteins', *Chem. Rev.* **1993**, *93*, 2833–2932.

[31] Bertini, I.; Luchinat, C.; Parigi, G., 'Magnetic susceptibility in paramagnetic NMR', *Prog. Nucl. Mag. Res. Sp.* **2002**, *40*, 249–273.

[32] Autschbach, J.; Patchkovskii, S.; Pritchard, B., 'Calculation of hyperfine tensors and paramagnetic NMR shifts using the relativistic zeroth-order regular approximation and density functional theory', *J. Chem. Theory Comput.* **2011**, *7*, 2175–2188.

[33] Charnock, G. T. P.; Kuprov, I., 'A partial differential equation for pseudocontact shift', *Phys. Chem. Chem. Phys.* **2014**, *16*, 20184–20189.

[34] McConnell, H. M., 'Indirect Hyperfine Interactions in the Paramagnetic Resonance Spectra of Aromatic Free Radicals', *J. Chem. Phys.* **1956**, *24*, 764.

[35] Rieger, P. H., *Electron spin resonance. Analysis and interpretation*, The Royal Society of Chemistry, Cambridge, UK, **2007**.

[36] Kaupp, M.; Köhler, F. H., 'Combining NMR spectroscopy and quantum chemistry as tools to quantify spin density distributions in molecular magnetic compounds', *Coord. Chem. Rev.* **2009**, *253*, 2376–2386.

[37] Neese, F., 'Prediction of molecular properties and molecular spectroscopy with density functional theory: From fundamental theory to exchange-coupling', *Coord. Chem. Rev.* **2009**, *253*, 526–563.

[38] Le Guennic, B.; Floyd, T.; Galan, B. R.; Autschbach, J.; Keister, J. B., 'Paramagnetic Effects on the NMR Spectra of "Diamagnetic" Ruthenium(bis-phosphine)(bissemiquinone) Complexes', *Inorg. Chem.* **2009**, *48*, 5504–5511.

[39] McConnell, H. M.; Holm, C. H., 'Proton Resonance Shifts in Nickelocene', *J. Chem. Phys.* **1957**, *27*, 314.

[40] McConnell, H. M.; Holm, C. H., 'Proton Resonance Shifts in Paramagnetic Metal Aromatic Complexes', *J. Chem. Phys.* **1958**, *28*, 749.

[41] Pritchard, B.; Autschbach, J., 'Theoretical Investigation of paramagnetic NMR Shifts in Transition Metal Acetylacetonato Complexes: Analysis of Signs, Magnitudes, and the Role of the Covalency of Ligand-Metal Bonding', *Inorg. Chem.* **2012**, *51*, 8340–8351.

[42] Autschbach, J.; Srebro, M., 'Delocalization error and 'functional tuning' in Kohn-Sham calculations of molecular properties', *Acc. Chem. Res.* **2014**, *47*, 2592–2602.

[43] Rastrelli, F.; Bagno, A., 'Predicting the NMR Spectra of Paramagnetic Molecules by DFT: Application to Organic Free Radicals and Transition-Metal Complexes', *Chem. Eur. J.* **2009**, *15*, 7990–8004.

[44] Rastrelli, F.; Bagno, A., 'Predicting the 1H and 13C NMR Spectra of Paramagnetic Ru(III) Complexes by DFT', *Magn. Reson. Chem.* **2010**, *48*, S132–S141.

[45] Clark, D. L.; Hobart, D. E.; Neu, M. P., 'Actinide Carbonate Complexes and Their Importance in Actinide Environmental Chemistry', *Chem. Rev.* **1995**, *95*, 25–48.

[46] Mizuoka, K.; Grenthe, I.; Ikeda, Y., 'Structural and Kinetic Studies on Uranyl(V) Carbonate Complex Using ^{13}C NMR Spectroscopy', *Inorg. Chem.* **2005**, *44*, 4472–4474.

[47] Gendron, F.; Pritchard, B.; Bolvin, H.; Autschbach, J., 'Magnetic Resonance Properties of Actinyl Carbonate Complexes and Plutonyl(VI)-tris-nitrate', *Inorg. Chem.* **2014**, *53*, 8577–8592.

[48] Gendron, F.; Páez-Hernández, D.; Notter, F.-P.; Pritchard, B.; Bolvin, H.; Autschbach, J., 'Magnetic properties and electronic structure of neptunyl^{VI} complexes: Wavefunctions, orbitals, and crystal-field models', *Chem. Eur. J.* **2014**, *20*, 7994–8011.

[49] Sharkas, K.; Pritchard, B.; Autschbach, J., 'Effects from spin-orbit coupling on electron-nucleus hyperfine coupling calculated at the restricted active space level for Kramers doublets', *J. Chem. Theory Comput.* **2015**, *11*, 538–549.

[50] Helgaker, T.; Coriani, S.; Jørgensen, P.; Kristensen, K.; Olsen, J.; Ruud, K., 'Recent Advances in Wave Function-Based Methods of Molecular-Property Calculations', *Chem. Rev.* **2012**, *112*, 543–631.

[51] Szalontai, G.; Csonka, R.; Speier, G.; Kaizer, J.; Sabolovíc, J., 'Solid-State NMR Study of Paramagnetic Bis(alaninato-κ^2N,O)copper(II) and Bis(1-amino(cyclo)alkane-1-carboxylato-κ^2N,O)copper(II) Complexes: Reflection of Stereoisomerism and Molecular Mobility in ^{13}C and ^{2}H Fast Magic Angle Spinning Spectra', *Inorg. Chem.* **2015**, *54*, 4663–4677.

[52] Kong, X.; Terskikh, V. V.; Khade, R. L.; Yang, L.; Rorick, A.; Zhang, Y.; He, P.; Huang, Y.; Wu, G., 'Solid-State ^{17}O NMR Spectroscopy of Paramagnetic Coordination Compounds', *Angew. Chem. Int. Ed.* **2015**, *54*, 4753–4757.

[53] Cheng, R.-J.; Ting, C.-H.; Chao, T.-C.; Tseng, T.-H.; Chen, P. P., 'The characterization of the saddle shaped nickel(III) porphyrin radical cation: an explicative NMR model for a ferromagnetically couSpectroscopy-porphyrin radical', *Chem. Commun.* **2014**, *50*, 14265–14268.

[54] Awais Rouf, S.; Mares, J.; Vaara, J., '^{1}H Chemical shifts in paramagnetic Co(II) pyrazolylborate complexes: A first-principles study', *J. Chem. Theory Comput.* **2015**, *11*, 1683–1691.

[55] Mares, J.; Hanni, M.; Lantto, P.; Lounila, J.; Vaara, J., 'Curie-type paramagnetic NMR relaxation in the aqueous solution of Ni(ii)', *Phys. Chem. Chem. Phys.* **2014**, *16*, 6916–6924.

[56] Mares, J.; Liimatainen, H.; Pennanen, T. O.; Vaara, J., 'Magnetic Properties of Ni2+(aq) from First Principles', *J. Chem. Theory Comput.* **2011**, *7*, 3248–3260.

[57] Fusaro, L.; Casella, G.; Bagno, A., 'Direct Detection of ^{17}O in [Gd(DOTA)]$^{-}$ by NMR Spectroscopy', *Chem. Eur. J.* **2015**, *21*, 1955–1960.

[58] Borgogno, A.; Rastrelli, F.; Bagno, A., 'Predicting the spin state of paramagnetic iron complexes by DFT calculation of proton NMR spectra', *Dalton Trans.* **2014**, *43*, 9486–9496.

[59] Rudolph, R.; Blom, B.; Yao, S.; Meier, F.; Bill, E.; van Gastel, M.; Lindenmaier, N.; Kaupp, M.; Driess, M., 'Synthesis, Reactivity, and Electronic Structure of a Bioinspired Heterobimetallic [Ni(μ-S_2)Fe] Complex with Disulfur Monoradical character', *Organometallics* **2014**, *33*, 3154–3162.

[60] Walton, J. W.; Carr, R.; Evans, N. H.; Funk, A. M.; Kenwright, A. M.; Parker, D.; Yufit, D. S.; Botta, M.; Pinto, S. D.; Wong, K.-L., 'Isostructural Series of Nine-Coordinate Chiral Lanthanide Complexes Based on Triazacyclononane', *Inorg. Chem.* **2012**, *51*, 8042–8056.

[61] Yamada, M.; Someya, C.; Wakahara, T.; Tsuchiya, T.; Maeda, Y.; Akasaka, T.; Yoza, K.; Horn, E.; Liu, M. T. H.; Mizorogi, N.; Nagase, S., 'Metal Atoms Collinear with the Spiro Carbon of 6,6-Open Adducts, $M_2@C_{80}$(Ad) (M = La and Ce, Ad = Adamantylidene)', *J. Am. Chem. Soc.* **2008**, *130*, 1171–1176.

[62] Yamada, M.; Wakahara, T.; Lian, Y.; Tsuchiya, T.; Akasaka, T.; Waelchli, M.; Mizorogi, N.; Nagase, S.; Kadish, K. M., 'Analysis of Lanthanide-Induced NMR Shifts of the Ce@C82 Anion', *J. Am. Chem. Soc.* **2006**, *128*, 1400–1401.

[63] Wang, X.; Zuo, T.; Olmstead, M. M.; Duchamp, J. C.; Glass, T. E.; Cromer, F.; Balch, A. L.; Dorn, H. C., 'Preparation and Structure of $CeSc_2N@C_{80}$: An Icosahedral Carbon Cage Enclosing an Acentric $CeSc_2N$ Unit with Buried f Electron Spin', *J. Am. Chem. Soc.* **2006**, *128*, 8884–8889.

[64] Reilley, C. N.; Good, B. W.; Desreux, J. F., 'Structure-independent method for dissecting contact and dipolar NMR shifts in lanthanide complexes and its use in structure determination', *Anal. Chem.* **1975**, *47*, 2110–2116.

[65] Di Pietro, S.; Piano, S. L.; Di Bari, L., 'Pseudocontact shifts in lanthanide complexes with variable crystal field parameters', *Coord. Chem. Rev.* **2011**, *255*, 2810–2820.

[66] Castro, G.; Bastida, R.; Macías, A.; Pérez-Lourido, P.; Platas-Iglesias, C.; Valencia, L., 'Lanthanide(III) Complexation with an Amide Derived Pyridinophane', *Inorg. Chem.* **2015**, *54*, 1671–1683.

[67] Martel, L.; Magnani, N.; Vigier, J.-F.; Boshoven, J.; Selfslag, C.; Farnan, I.; Griveau, J.-C.; Somers, J.; Fanghänel, T., 'High-Resolution Solid-State Oxygen-17 NMR of Actinide-Bearing Compounds: An Insight into the 5f Chemistry', *Inorg. Chem.* **2014**, *53*, 6928–6933.

[68] Magnani, N.; Santini, P.; Amoretti, G.; Caciuffo, R., 'Perturbative approach to $\boldsymbol{J}$ mixing in f-electron systems: Application to actinide dioxides', *Phys. Rev. B* **2005**, *71*, 054405 (7 pages).